Feasibility Study of Using the Housing Cases of Implantable Devices as Antennas

Muayad Kod, Jiafeng Zhou, *Member, IEEE*, Yi Huang, *Senior Member, IEEE*, Manoj Stanley, Muaad Hussein, Abed P. Sohrab, Rula Alrawashdeh and Guozheng Wang

***Abstract*— A novel antenna design for implantable pacemakers is proposed. The housing of a pacemaker is utilized as an antenna to cover both the 402-405 MHz MICS (Medical Implant Communication Service) band and the 433 MHz ISM (Industrial, Scientific and Medical) band. This is achieved by exploiting radiating characteristic current modes of the housing case. These modes are excited using a capacitive coupling element with the help of a matching circuit. The radiation pattern of this antenna is optimized to be in a desirable direction away from the body (off-body direction). The ability of the proposed antenna for communications is demonstrated using a transceiver and a base station at 433 MHz. A communication range of 1 m is established when a transmitter with the proposed antenna is implanted in a rabbit and the power fed by the transceiver to the antenna is 25 µW. A longer range of up to 19 m can be established with the maximum allowable transmit power within the safety limits. Furthermore, the far field wireless power transfer (WPT) through the proposed antenna is investigated by experiment. A received power of up to 22.38 µW by the proposed antenna is demonstrated when an equivalent isotropically radiated power (EIRP) of 140 mW is transmitted 1 m away from a transmitting antenna. From the same transmitting antenna in the same distance, a power of 2.2 mW can be received when the transmit power is within safety limits. This power can be used to recharge a small battery or a capacitor which can potentially cover the communication power consumption of the pacemaker and hence extend the life span of the primary battery.**

***Index Terms*— housing antenna, MICS band antenna, pacemaker**

I. INTRODUCTION

PACEMAKER is an important implantable device that is used to monitor and regulate heartbeats. It is implanted in the chest area under skin and enclosed normally inside a metal case. The case is usually made of biocompatible conducting material such as Titanium. Traditionally, the device communicates with an external programmer through near field magnetic coupling. This is mainly done by using coils at low frequencies at several kilohertz [1, 2]. In 1999, the U.S. Federal Communications Commission (FCC) allocated the Medical Implant Communication Service (MICS) band (402 – 405 MHz) to permit the use of a mobile radio device for data communication for implantable devices as a response to petition from Medtronic [3]. By using the RF band, the range to establish a communication link with implantable devices can be significantly extended [4]. The equivalent isotropically radiated power (EIRP) of MICS devices is limited to -16 dBm to restrain the interference to other medical devices [5]. This band is later adopted by European Telecommunications Standards Institute (ETSI) in 2002 and become the target band for implantable antenna designers [6].

The conducting material of the case of an implantable device, such as a pacemaker, can attenuate electromagnetic RF signals significantly so that implantable RF antennas could not be totally placed inside the case. A significant amount of work has been done to design RF antennas for implantable devices. A loop antenna was proposed to work at MICS band and embedded inside the header of the pacemaker [7]. A microstrip antenna was proposed to be attached to the pacemaker case but this adds extra thickness to the pacemaker profile [8]. A PIFA antenna working at the MICS band was placed at the surface side of the pacemaker by considering the housing case as ground plane. The same group designed another PIFA but this time it was placed at the top side of the pacemaker [9, 10]. In both cases, the implant size is increased. In another study, an inverted-E antenna is proposed to be embedded to the pacemaker header [11].

A monopole antenna has been investigated for the pacemaker RF telemetry. The monopole was proposed with a folded shape to get the required length for resonance at the desired band. It was embedded to the pacemaker header in [12]. A helical monopole antenna was proposed to be embedded in the pacemaker header as well. With the increase of the helix turns, a desired length of quarter wavelength can be obtained [13]. A circumference monopole antenna was proposed in [14]. This monopole was rotated around the pacemaker case. An optional telemetry antenna is proposed in [15]. This antenna looked like a monopole and had a connection end with the electrode lead of the pacemaker. It can be utilized as an antenna by itself as the authors suggested or in collaboration with another existing telemetry antenna. These previous designs added extra elements to the implant that would increase the size and complexity of implantable devices.

A slot antenna was investigated as well for the pacemaker. A slot was made at one side of the case in [16]. The length of the slot can be increased to adapt the desired band. However, the physical length of the slot mainly determines the resonant frequency of the antenna and most power is radiated in the slot region.

Manuscript received 2016.

M. Kod, J. Zhou, Y. Huang, M. Hussein, A. P. Sohrab, and M. Stanly are with the Department of Electrical Engineering and Electronics, The University of Liverpool, Liverpool L69 3GJ, U.K. (e-mail:M.S.Kod@liv.ac.uk; Jiafeng.Zhou@liv.ac.uk; Yi.Huang@ieee.org).

In this paper, an approach to design an antenna using the housing case of implantable devices is presented for the first time. This design exploits the radiating characteristic current modes of the case to create a radiating antenna from the housing case itself at the frequency bands of interest. The radiating current modes are excited using a capacitive coupling element aided by a matching circuit. The proposed antenna has a radiation pattern that is outgoing from the housing case in normal direction to the pacemaker surface, which is very suitable for implantable devices as will be explained in the following sections.

The paper is organized as follows. In Section II, the antenna design and performance analysis are presented. Then, the wireless power transfer (WPT) to the implantable device is investigated using the proposed antenna in Section III. Section IV focuses on the communication experiment by using a transceiver with a temperature sensor. The paper is finally concluded in Section V.

II. Antenna Design and Performance Analysis

From the original shape of the pacemaker, a cavity with a small slot on the top side can be recognized as shown in Fig. 1(a). This small slot is reserved for lead electrodes to pass through into the pacemaker circuitry. The slot can be potentially used as an antenna. The characteristics of the slot antenna depend on the dimensions of the slot. Typically, the length of the slot is about half wavelength for resonance. The average length of the top side of a typical pacemaker is about 30 mm. The slot within this side could be widened up to 26 mm so that a margin metal of width 2 mm can be kept for header contact and insulation as shown in Fig. 1(b). A rectangular box is considered in this study to approximate a commercial pacemaker and also for easy to fabricate as shown in Fig. 1(c). The same design method could also be applied to other implantable devices with different cavity shapes.

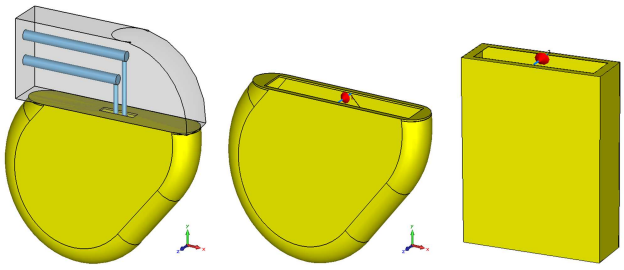

(a) (b) (c)

Fig. 1. The pacemaker housing antenna (a) The structure of a pacemaker (b) Creating a slot from the pacemaker's housing case and (c) A rectangular box shape slot antenna to validate the approach for easy fabrication.

The reflection coefficient S11 of both structures in the original shape and the rectangular shape is simulated using CST microwave studio. It shows that the two structures are resonating at 5.6 GHz which is equivalent to the slot size of 26 mm at a half wavelength as shown in Fig. 2. The simulation confirmed the relationship between the resonance and the slot length. Since the target frequency of implantable devices is in the MICS band, the radiating frequency of the slot antenna is too high with this dimension. More importantly, for a slot antenna, most power is radiated in the slot region, which is unfavorable for pacemaker applications since most power will be radiated to the body rather than off body as illustrated by the radiation pattern shown in Fig. 3.

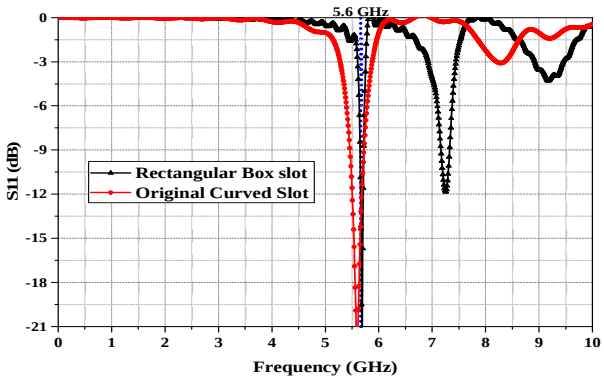

Fig. 2. The reflection coefficient S_{11} of the slot antenna in two cases: the original pacemaker curved shape and the rectangular box shape.

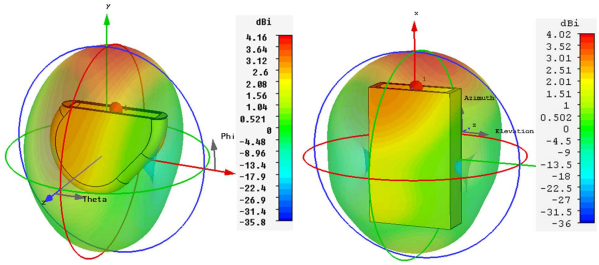

Fig. 3. The radiation pattern of the slot antenna at 5.6 GHz in the two cases: the original pacemaker shape and the rectangular box shape.

One of the techniques that have been adopted to the design of RF antennas recently is to create an antenna by utilizing a large ground plane or chassis by exploiting the characteristic current modes. The surface current distribution of conducting planes or chassis is constructed from infinite orthogonal characteristics current modes [17]. The radiation current modes of the chassis can be explored using the Theory of Characteristic Mode (TCM) analysis. The principle of TCM is explained well in [17, 18]. This approach of antenna design is mainly investigated for mobile terminals [18-20].

For a specific conducting surface, the current density J is given by

$$J = \sum_n \alpha_n J_n \tag{1}$$

where J_n represents the characteristic current modes, these characteristics mode currents are able to radiate power independently from each other [18]. α_n is the associated weighting coefficient of the current mode and it is related to

the excitation modal and eigenvalues as:

$$\alpha_n \propto \frac{V_n}{1+j\lambda_n} \tag{2}$$

where V_n is the excitation coefficient which denotes the applied excitation coupling to the current mode, the phase and magnitude of V_n affect the contribution of the current mode on the whole current distribution [17]. λ_n is the eigenvalue related to the current mode. The current density can be then given by

$$J = \sum_n \frac{V_n}{1+j\lambda_n} J_n \tag{3}$$

From equation (3) it can be seen that the current density is proportional to the eigenvalues and it is taking into account the excitation state of V_n in terms of phase and magnitude. The radiation characteristics of any specific current mode can be estimated by the associated eigenvalue λ_n. Whenever this value is close to zero, the current mode radiates. The magnitude of the term $\left|\frac{1}{1+j\lambda_n}\right|$ can be used to analyze the current mode rather than the individual eigenvalues. This term represent the normalized value of the current mode and is called modal significance (MS) [18]. The MS does not depend on the excitation and but is determined by the shape and size of the conducting surface [18].

Previous studies utilized ground planes to be effective radiative antennas for mobile terminals using simple and non-resonance coupling elements with the help of an external matching circuit [19, 21]. In this study, the housing of a pacemaker is considered as a kind of chassis with a cavity structure. The radiation characteristics from the housing itself will be investigated using this approach. The housing case is analyzed by TCM analysis in free space using FEKO software. The ISM band around 2.45 GHz is investigated since the dimension of cavity is comparable with the wavelengths at this band. The modal significance (MS) method is used to exploit the radiative current modes. This MS, the magnitude of $\left|\frac{1}{1+j\lambda_n}\right|$ as given in (3), has a maximum value of 1. Whenever its value is close to one then the current mode can effectively contribute in radiation [18].

The result of the TCM analysis for the proposed antenna is shown in Fig. 4. It can be seen from this figure, the first two modes have the highest MS at 2.45 GHz and in particular the first mode has an MS very close to 1. Mode 4 is dominant at the bands above 2.5 GHz. The surface currents associated with the first two modes are shown in Fig. 5. The current distribution of the first mode is longitudinal with the cavity surface and has high current density at the top side slot. The second mode is latitudinal on the surface including the area of the slot. The best excitation places for the current modes are at the maxima of the current distribution [17].

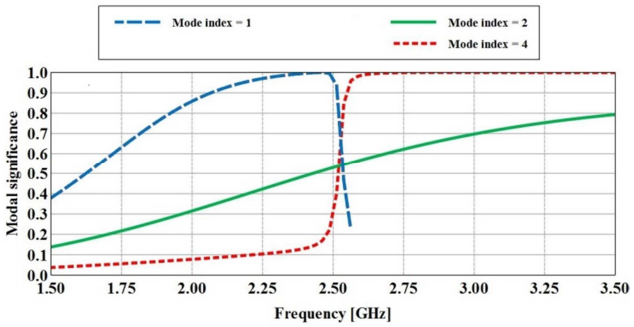

Fig. 4. Characteristic mode analysis of the proposed antenna in the rectangular box shape.

Since the dominant modes at this band have dense currents at the top slot side, the excitation would be useful at this position. The current modes have symmetric distribution around the cavity surface so that the excitation at the middle position of the slot will provide balanced excitation to the current modes. To excite the current modes of the housing at 2.45 GHz, a coupling element is used with the cavity. To avoid adding extra element to the pacemaker and keep the shape of the opening of the case as original, an element part is cut from the top side of the housing cavity as shown in Fig. 6.

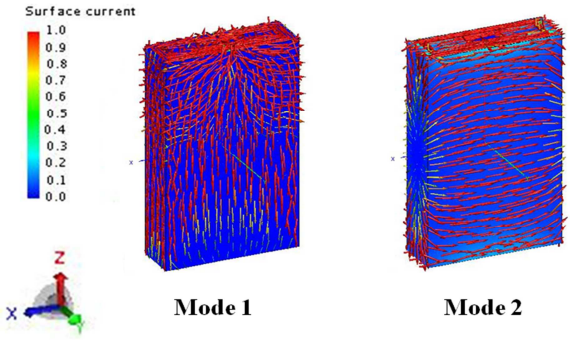

Fig. 5. The current distribution of the first three mode of the proposed housing antenna.

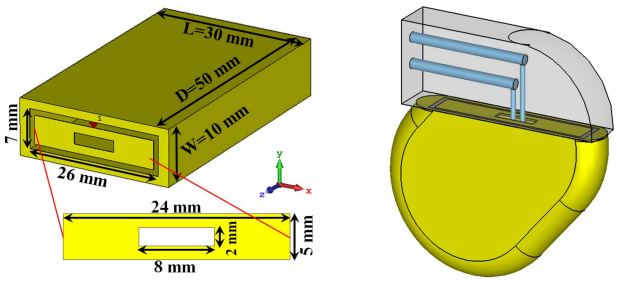

(a) (b)

Fig. 6. The propsed antenna (a) Dimension details of the proposed rectangular box antenna (b) the proposed antenna in the original pacemaker shape.

A tiny slot with the dimensions of 2 mm × 8 mm is placed at the center of the coupling element for the original usage of pacemaker to lead electrode to pass-through to the internal circuit as shown in Fig. 6(b). This slot has negligible effect on the antenna performance. The proposed antenna has the same shape and dimension as the slot antenna except the added coupling element. The performance of both antennas are simulated and compared. It is worth mentioning that the dimensions of this box have been chosen so that it is close to the dimension of the original pacemaker and also to fit a transceiver circuit that will be used in the following sections to test the communication ability of the proposed antenna. The proposed housing antenna with the coupling element is simulated and compared with the slot antennas. The housing antenna has a resonance similar to the slot antenna but the resonance is shifted to a slightly lower frequency as shown in Fig. 7. The performance of the antenna around the resonant frequency of 5.6 GHz has been changed slightly mainly due to the capacitive effect of the coupling element.

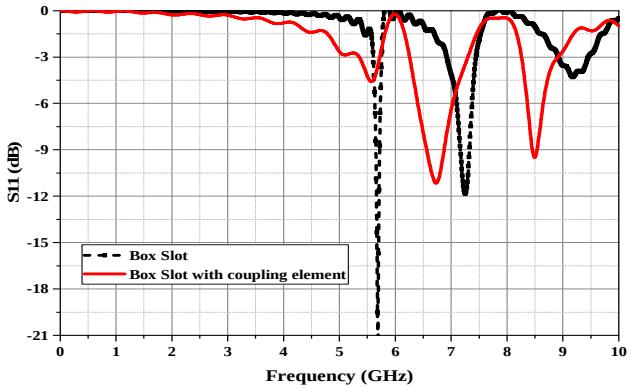

Fig. 7. Comparison of the reflection coefficient S_{11} of the rectangular box in the proposed housing antenna design and the slot antenna design.

Then an external matching circuit is applied to the coupling element to excite the modes at 2.45 GHz. The matching circuit can be designed automatically using CST with connection to specialist software in designing matching circuit such as Optenni lab. This software has libraries of real commercial components. The matching circuit is designed using this software based on the imported file from CST with flexibility to choose the order and topology of the circuit. The designed circuit is imported back to the CST to be attached to the antenna port. The reflection coefficient of the antenna after adding L-matching circuit is shown in Fig. 8. It has 28 MHz bandwidth at -10 dB return loss. The gain of the proposed antenna at this band is 2.59 dB and the total radiation efficiency is 75%. The total antenna efficiency is slightly low due to the use of the matching circuit. A matching circuit is produced at 2.45 GHz and applied to the slot antenna to find out the difference in performance as compared with the proposed one.

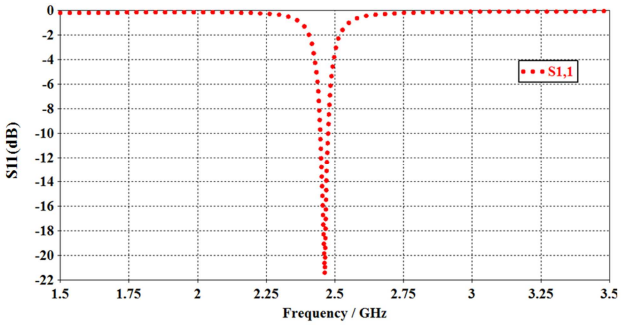

Fig. 8. The reflection coefficient S11 of the housing antenna at 2.45 GHz after adding the matching circuit to the coupling element.

The matching circuits and surface current distributions of the housing antenna with the coupling element and the slot antenna are shown in Fig. 9. The radiative current modes at 2.45 GHz have been excited successfully using the coupling element as shown in Fig. 9(a). As a result, the surface current along the sides of the case is activated which is associated with the first and third current modes. While the surface current in the middle for the front face is mostly related to the second mode. These surface currents will participate in forming the radiation pattern. On other hand, the surface current of the slot antenna is mostly distributed along the slot aperture. As a result, the radiation will be generated mainly from the slot aperture itself as shown in Fig. 9(b).

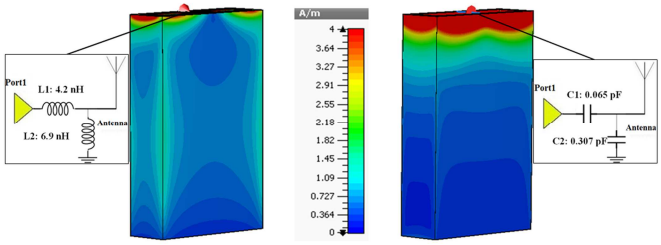

(a) (b)

Fig. 9. Matching circuit and surface current at 2.45 GHz of (a) the proposed housing antenna (b) the slot antenna.

This excitation of the proposed antenna results in radiation from the housing case itself with a radiation pattern perpendicular to the housing surface as shown in Fig. 10(a) and (b). The reason for radiation mainly in one direction is the unbalanced excitation to the cavity surface where the feeding is applied between one side of the cavity and the coupling element. On contrast, the radiation of the slot antenna is still mainly from the slot aperture as shown in Fig. 10(c) and (d). The proposed design has significant advantage over the performance of the equivalent slot antenna in terms of radiation from the housing itself with radiation pattern going away from the pacemaker off the body. This design represents an advantage for the pacemaker application due to the flexibility to choose the desired band and can generate the desired radiation pattern.

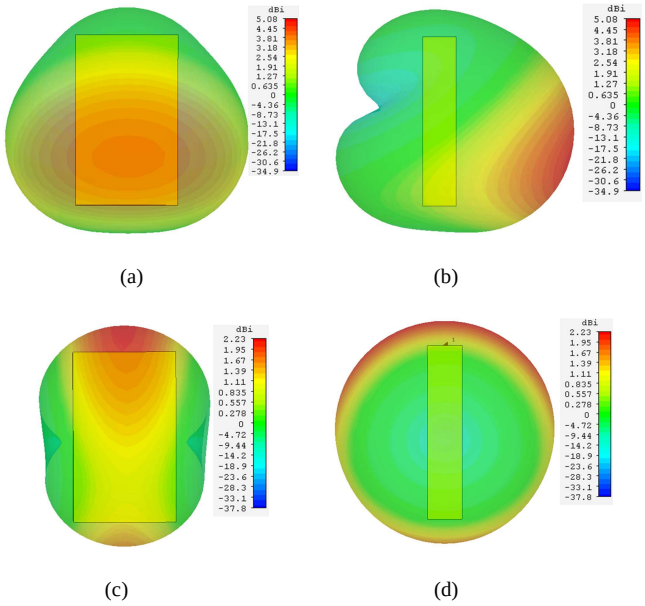

Fig. 10. Radiation pattern at 2.45 GHz with a matching circuit. (a) Front view of the proposed antenna (b) Side view of the proposed antenna (c) Front view of the slot antenna (b) Side view of the slot antenna.

Since the pacemaker is used inside a human body, the properties of the housing antenna are investigated with the presence of body tissues. The high dielectric properties of the body tissues change the antenna performance. The resonance frequency inside the body is related to the free space resonant frequency according to the properties of the tissue and is given by

$$f_r = \frac{f_0}{\sqrt{\varepsilon_e}} \tag{4}$$

where f_0 is the resonant frequency in free space, f_r is the resonant frequency in the body medium and ε_e is the relative equivalent effective permittivity of that medium. The resonant frequency of the antenna will move down to a lower value due to the effect of body tissues. The body tissue properties in terms of dielectric constant at 403 MHz are 57.1, 11.6 and 46.7 for muscle, fat and skin, respectively.

The same procedure that was done in free space is then carried out to the housing antenna with the coupling element in the body model. The coupling element with the matching circuit is used to excite the current modes of the antenna at the MICS band. The simulation results confirm that the principle of performance is similar to that in free space. The surface current is activated on the case antenna surface with most power radiated in the direction perpendicular to the front surface of the antenna as shown in Fig. 11. To validate this design, the housing case is fabricated by cutting 0.1 mm copper sheet into shape. The coupling element is fabricated on a 0.57 mm thick FR4 substrate. Then a T-matching network circuit is constructed on the coupling element as shown in Fig. 12.

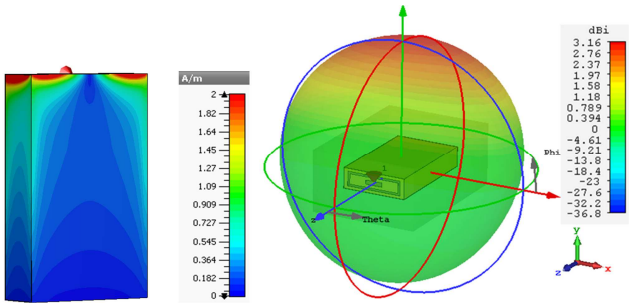

Fig. 11. Simulated surface current and radiation pattern of the proposed antenna at 403 MHz.

Minced pork is used as a mimic to human tissues to test the proposed antenna. The reflection coefficient S11 of the prototype antenna is measured using a portable VNA as shown in Fig. 13.

The antenna response has a good agreement with the simulated results as shown in Fig. 14. From the figure, it can be shown that a very small frequency shift is encountered due to fabrication precision. However, it still covers the desired bands of the MICS band and the ISM band at 433 MHz. The proposed antenna is investigated in terms of the effect of pacemaker parts including the battery and the PCB board. It is found that the resonance is slightly shifted of 14 MHz but the desired bands are still covered. Furthermore, this slightly shift can be compensated by tuning the matching circuit.

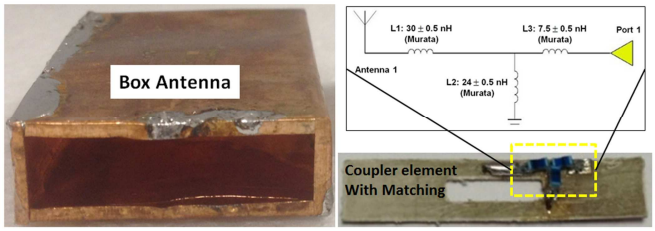

Fig. 12. The fabricated prototype of the proposed antenna and the matching circuit.

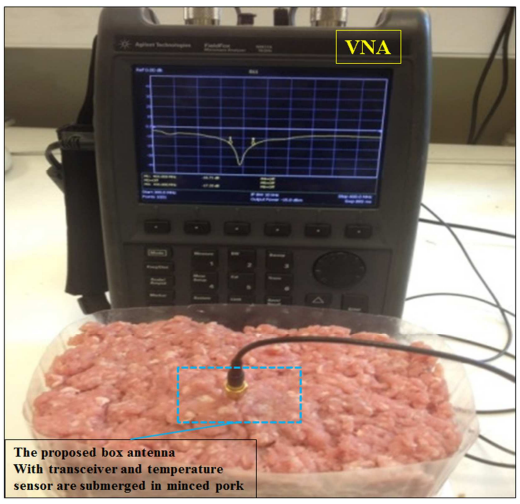

Fig. 13. The S_{11} measurement setup of the proposed housing antenna inside minced pork

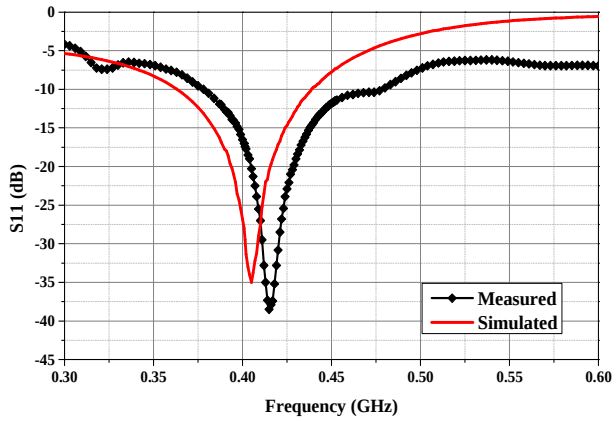

Fig. 14. The simulated and measured S_{11} of the proposed rectangular box antenna.

The simulation results of the proposed antenna also show that the realized gain and radiation efficiency are -30 dB, 0.038% and -30.1, 0.04% dB at 433 MHz and 403 MHz, respectively. These values are relatively small as expected due to the large loss of human body tissues [22]. Nonetheless, these values are enough to build up a communication link over 1 m when the power fed by the transceiver to the antenna is 25 µW. A longer range of up to 19 m can also be established with a larger transmit power within the safety limits as will be shown in the following sections.

III. Wireless Power Transfer

The proposed housing case antenna is tested for WPT. The experiment of far field WPT is done inside the anechoic chamber as shown in Fig. 15. The experiment setup includes a signal generator, a power amplifier to boost the transmit power with a gain of 53 dB, a transmitting antenna, a wideband power sensor and a laptop to read the received power. The proposed antenna is tested inside two different body phantoms: minced pork and a rabbit. The transmitting antenna is a meandered loop resonating at 433 MHz in free space with a gain of 2.3 dB and a radiation efficiency of 96%. It is worth mentioning that there is a measurement error of 1 dB in all measurement results. This experiment is carried out in two scenarios.

A. Experiment in Minced Pork

Minced pork that mimics human tissues is used to test the proposed antenna for WPT. In the receiving side, the antenna is buried in the pork. The thickness of the pork between the case and the pork container is 2 cm. The received power by the antenna is fed to a power sensor that is connected to a laptop to read the power level. The transmitting side includes the signal generator that feeds a power amplifier. The output of the amplifier feeds the transmitting loop antenna.

An EIRP of 140 mW was transmitted during the experiment. The received power by the antenna is measured with several distances as shown in Fig. 16. In the near field region of the antenna, smaller steps of measurement are used for higher accuracy. At the distance of 1 m, the received power was 6.2 µW when the transmit power is 140 mW.

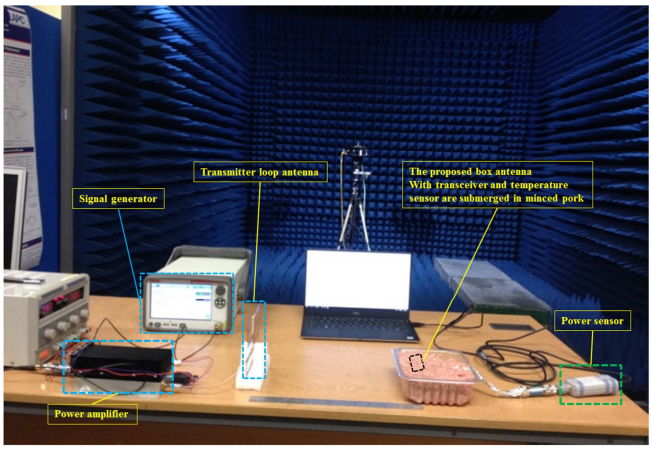

Fig. 15. The experiment setup of the WPT using the proposed antenna in minced pork inside an anechoic chamber.

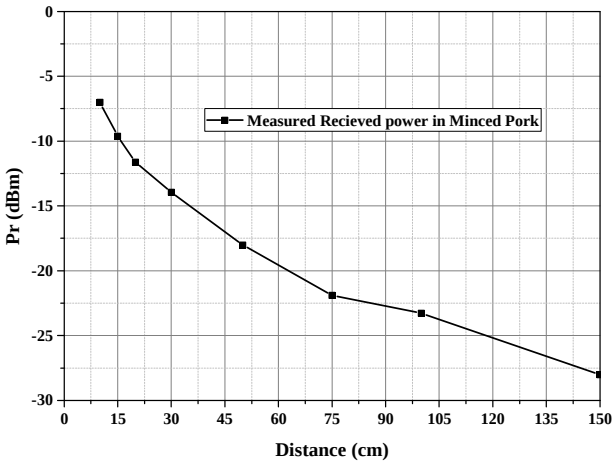

Fig. 16. The measured received power in minced pork with respect to distance. The EIRP transmit power is 140 mW.

To measure the received power at several misalignment angles, the proposed antenna and the transmitting antenna are kept apart for 1 m. Then the transmitting antenna is rotated around the azimuth in several angles of 15˚ then 30˚, 45˚ and 60˚. The proposed receiving antenna is facing the center location of the transmitting antenna at all angles. Since the transmitting antenna is symmetrical, the received power at other symmetrical angles, namely -15˚, -30˚, -45˚ and -60˚, is assumed to be the same. The measured results are shown in Fig. 17. The received power dropped from 6.2 µW to 1.3 µW due to the misalignment angle between the main beams of the antennas. The received power in both cases: versus the distance and versus the angle misalignment shows a good agreement with the predicted responses by simulation as shown in Fig. 16 and Fig. 17.

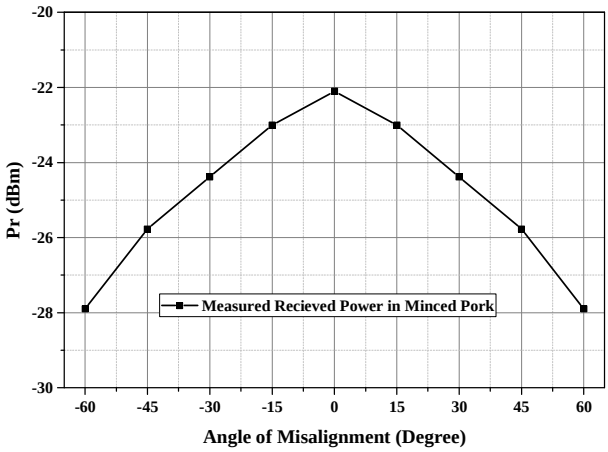

Fig. 17. The measured received power in minced pork with respect to rotation angle at a separation distance of 1 m between the transmitting and receiving antennas. The EIRP transmitted is 140 mW.

B. *Experiment in a Rabbit*

A 3 Kg male New Zealand type of rabbit was purchased from Envigo. The rabbit was maintained in a lab for 10 days and prepared following Schedule 1 for the experiment. The WPT experiment is carried out with the same setup as in the minced pork. The proposed antenna is implanted under the skin in the chest region of the rabbit. The antenna is connected using a micro coaxial cable to the power sensor to read the received power. In the experiment, the proposed antenna is tested in two orientations: horizontal for the scenario when a patient is standing and vertical for the scenario when a patient is sleeping. The measurement is done first to find out the received power level at different separation distances from the transmitting antenna. The received power versus the separation range is depicted in Fig. 18.

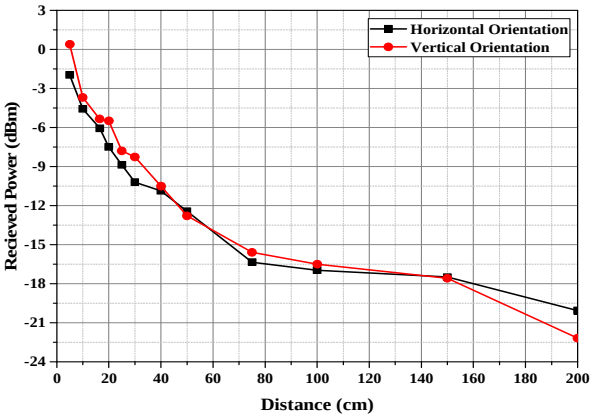

Fig. 18. The received power versus distance measured using the proposed antenna in a rabbit. The EIRP transmitted is 140 mW.

It can be seen from Fig. 18 that both orientations have similar receiving response with a slightly higher power in the vertical orientation. This advantage is counted to the proposed antenna where it can receive efficiently in two orientations. The power received at 1 m distance was 22.38 µW and 20.1 µW at the vertical and horizontal orientations, respectively. The transmit EIRP during the experiment was kept at 140 mW.

An experiment was then carried out to investigate the received power in different angles. Since the receiving antenna is embedded under the rabbit skin, it is kept in the same position and the angle of the transmitting antenna was rotated with respect to its azimuth from −60˚ to +60˚ with a rotation step of 15˚. The experiment is carried out for both horizontal and vertical orientations as shown in Fig. 19. The received power was not symmetrical because the radiation pattern of the receiving antenna is not symmetrical in the vertical direction as shown in Fig. 10 (a) and (b) and Fig. 11.

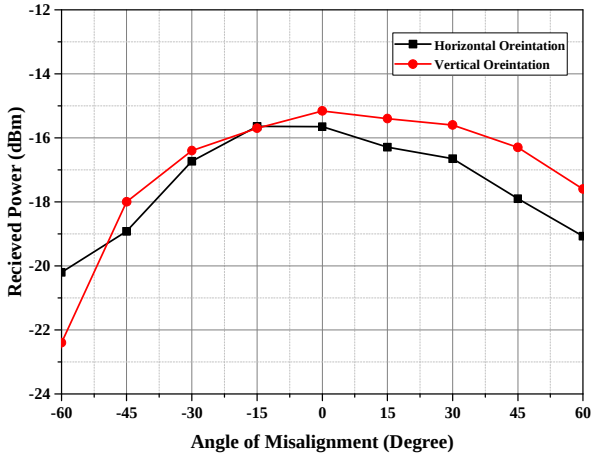

Fig. 19. The received power versus rotation angle measured in a rabbit with separation distance of 1 m between the transmitting and receiving antennas.

C. *Maximum Exposure Limits*

In this section, the maximum transmit power by the transmitting antenna for far field WPT will be discussed according to the maximum exposure safety limits. According to IEEE standards for maximum exposure limits, the maximum power density at the body is 13.4 W/m² in the controlled environment and 2 W/m² in the public environment [23]. The far field power density from a transmitting antenna is given by

$$S = \frac{P_T\, G_T}{4\pi R^2} \tag{5}$$

where S is the power density in W/m^2, P_T is the transmitted power by the antenna in watt, G_T is the gain of the transmitting antenna and R is the distance in meters from the transmitting antenna to the destination. The gain of the transmitting antenna in the experiment was 2.3 dB.

The maximum allowed EIRP at 1 m away from the transmitter in a public environment is 14.7 W. With this level of transmitted power, 2.2 mW can be received using the proposed antenna in the rabbit experiment and 0.62 mW in the minced pork experiment.

IV. COMMUNICATION MEASUREMENT

To demonstrate the ability of the proposed antenna for establishing a communication link, an experiment using a transceiver has been carried out. This transceiver is a part of a wireless temperature station. It has a temperature sensor and the transceiver works at 433.9 MHz. The proposed antenna covers both the MICS band of 402-405 MHz and the ISM band at 433 MHz. The proposed antenna was used in the experiment to work at 433.9 MHz.

The wireless weather Station has two parts: an indoor reader station that has a monopole receiving antenna with gain of 1.38 dB and an outdoor transmitting tag that contains a temperature sensor and an antenna with a gain of 1 dB, both at 433.9 MHz. The outdoor tag is modified so that the original antenna is replaced with the proposed one. The modified transceiver can be fitted inside the box as shown in Fig. 20. The transmit power of the tag transceiver is found out to be 25 µW. The modified communication system is demonstrated in vivo as follows:

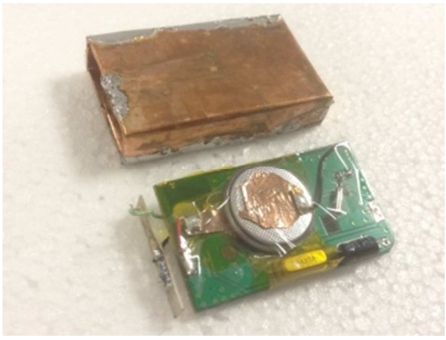

Fig. 20. The modified transceiver to be fit inside the proposed box antenna.

A. Experiment in Minced Pork and a Rabbit

The experiment setup includes the proposed antenna with the modified transmitter tested first in minced pork. A receiver station is used to read out the temperature. The experiment setup is shown in Fig. 21. It is worth mentioning that the antenna was totally submerged in the minced pork during the experiment. The antenna can be seen in Fig. 20 just to show where the antenna was placed.

The temperature can be read within a range of 32 cm with the default transceiver transmit power of 25 µW. A longer range is expected if the transmit power is boosted to higher levels but within the safety limits. The receiving system can also be improved to increase the range. The result has verified that the proposed antenna can be used for effective communication.

The same experiment of communication is carried out in a rabbit as well. The housing antenna with the transceiver is implanted under the skin of the rabbit. A communication range of 1 m is achieved. The improved range is a consequence of the thin layer of the rabbit skin as compared with the 2 cm thick minced pork.

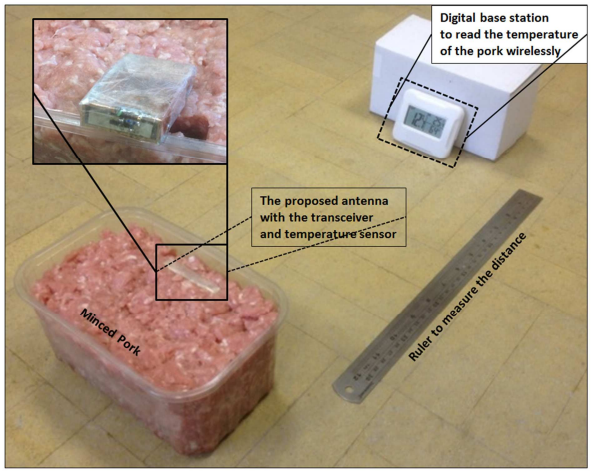

Fig. 21. The communication experiment of the proposed antenna to read the temperature in minced pork.

B. Specific Absorption Rate

The Specific Absorption Rate (SAR) is an essential factor to measure the absorbed power by the tissue [24]. It is primarily determined by the electric field as given by

$$SAR = \frac{\sigma |E|^2}{\rho} \tag{6}$$

where ρ (kg/m^3) is the mass density, σ (S/m) is the conductivity of the tissue and $|E|$ (V/m) is the magnitude of the electric field .

The proposed antenna can be used for communication as verified by the experiment. The maximum transmit power from the proposed implanted antenna within the safety regulations can be computed according to the SAR. The FCC SAR regulation of 1.6 W/kg per 1-g averaging was considered to determine the usability of the proposed antenna. It is found by calculating the SAR using CST studio that the proposed design can be used with a transmission power of up to 9 mW. The experiment of communication is carried out with a transmit power of 25 µW which is fixed in the transmitter module. A communication range of 32 cm and 1 m is achieved inside minced pork and a rabbit respectively. Longer range is achievable with this antenna by increasing the transmit power up to 9 mW. By feeding the proposed antenna with this higher transmit power, it is estimated by calculation that a communication range of up to 19 m can be established.

V. CONCLUSION

This paper has presented a novel antenna design using the housing case of a pacemaker. The proposed concept can be used for many other implantable devices with a conducting case. This housing antenna is optimized to work at the ISM

band around 2.45 GHz in free space and then is optimized at the MICS band of 402 – 405 MHz and the ISM band around 433 MHz. This design offers a radiation pattern that is going out of the housing surface and off the body. It is suitable for implantable devices such as pacemakers due to the flexibility to choose the desired frequency band and a suitable radiation pattern.

The proposed antenna is tested for establishing communication links. This system established a communication link distance of 32 cm when the system was placed inside minced pork. The same experiment is carried out inside a rabbit and a communication range of 1 m has been achieved. This antenna can cover further range with a higher transmit power and still within the safety limits.

A wireless power transfer experiment is also done to find out the capability of the proposed antenna for energy harvesting. The experiment shows promising results. A received power of 22.4 μW is demonstrated when an EIRP of 140 mW is transmitted from an antenna 1 m away. By boosting the transmitter with higher power but within safety limits, a power of 2.2 mW can be received from the same distance. The received power can be potentially used to recharge a small battery.

If this design is implemented in a pacemaker, it can provide energy for communication and reserve the energy of the primary battery solely for the core function of the pacemaker. For long term of operation that is typically 5-7 years, this amount of reserved energy could be significant and help in extending the lifespan of the primary battery.

ACKNOWLEDGMENT

We would like to thank Dr. Mark Hall in Liverpool Heart and Chest Hospital, UK for his discussion and providing samples.

REFERENCES

[1] P. Arzuaga, "Cardiac Pacemakers: Past, Present and Future," *Ieee Instrumentation & Measurement Magazine*, vol. 17, pp. 21-27, Jun 2014.

[2] A. J. Shah, J. D. Brunett, J. P. Thaker, M. B. Patel, V. V. Liepa, K. Jongnarangsin, *et al.*, "Characteristics of telemetry interference with pacemakers caused by digital media players," *Pacing and Clinical Electrophysiology*, vol. 33, pp. 712-720, 2010.

[3] H. D. Marlene, "FCC-03-32A1," *Federal Communications Commission Office of Engineering & Technology*, 2003.

[4] K. S. Nikita, *Handbook of biomedical telemetry*: John Wiley & Sons, 2014.

[5] H. S. Savci, A. Sula, Z. Wang, N. S. Dogan, and E. Arvas, "MICS transceivers: Regulatory standards and applications," *Proceedings of the IEEE SoutheastCon 2004*, pp. 179-182, 2005.

[6] E. T. S. Institute, "Ultra Low Power Active Medical Implants (ULP-AMI) and Peripherals (ULP-AMI-P) operating in the frequency range 402 MHz to 405 MHz," 2009.

[7] F. C. W. Po, C. Delavaud, E. de Foucauld, J.-B. David, and P. Ciais, *An Efficient Adaptive Antenna-Impedance Tuning Unit Designed for Wireless Pacemaker Telemetry*: INTECH Open Access Publisher, 2011.

[8] W. Huang and A. A. Kishk, "Embedded Spiral Microstrip Implantable Antenna," *International Journal of Antennas and Propagation*, 2011.

[9] T. Houzen, M. Takahashi, and K. Ito, "Implanted antenna for an artificial cardiac pacemaker system," *Piers 2007 Prague: Progress in Electromagnetics Research Symposium, Proceedings*, pp. 51-54, 2007.

[10] S. Lee, W. Seo, K. Ito, and J. Choi, "Design of an implanted compact antenna for an artificial cardiac pacemaker system," *Ieice Electronics Express*, vol. 8, pp. 2112-2117, Dec 25 2011.

[11] P. Li, G. A. Mouchawar, J. Amely-Velez, and R. Imani, "Inverted E antenna with capacitance loading for use with an implantable medical device," ed: Google Patents, 2015.

[12] S. Vajha, K. R. Maile, D. E. Larson, D. A. Chizek, and J. M. Edgell, "Folded antennas for implantable medical devices," ed: Google Patents, 2011.

[13] J. A. Von Arx, W. R. Mass, S. T. Mazar, and M. D. Amundson, "Antenna for an implantable medical device," ed: Google Patents, 2009.

[14] M. D. Amundson, J. A. Von Arx, W. J. Linder, P. Rawat, and W. R. Mass, "Circumferential antenna for an implantable medical device," ed: Google Patents, 2004.

[15] G. L. Dublin, W. D. Verhoef, and R. S. Wallace, "Optional telemetry antenna for implantable medical devices," ed: Google Patents, 2008.

[16] D. Aghassian, L. Freidin, and V. Dronov, "Implantable Medical Device Having A Slot Antenna In Its Case," ed: Google Patents, 2008.

[17] R. Martens and D. Manteuffel, "Systematic design method of a mobile multiple antenna system using the theory of characteristic modes," *IET Microwaves, Antennas & Propagation*, vol. 8, pp. 887-893, 2014.

[18] M. Cabedo-Fabres, E. Antonino-Daviu, A. Valero-Nogueira, and M. F. Bataller, "The Theory of Characteristic Modes Revisited: A Contribution to the Design of Antennas for Modern Applications," *IEEE Antennas and Propagation Magazine*, vol. 49, pp. 52-68, 2007.

[19] R. Valkonen, M. Kaltiokallio, and C. Icheln, "Capacitive Coupling Element Antennas for Multi-Standard Mobile Handsets," *Ieee Transactions on Antennas and Propagation*, vol. 61, pp. 2783-2791, May 2013.

[20] J. Villanen, J. Ollikainen, O. Kivekas, and P. Vainikainen, "Coupling element based mobile terminal antenna structures," *IEEE Transactions on Antennas and Propagation*, vol. 54, pp. 2142-2153, 2006.

[21] J. Holopainen, R. Valkonen, O. Kivekas, J. Ilvonen, and P. Vainikainen, "Broadband Equivalent Circuit Model for Capacitive Coupling Element-Based Mobile Terminal Antenna," *Ieee Antennas and Wireless Propagation Letters*, vol. 9, pp. 716-719, 2010.

[22] Z. Duan, Y. X. Guo, M. Y. Je, and D. L. Kwong, "Design and in Vitro Test of a Differentially Fed Dual-Band Implantable Antenna Operating at MICS and ISM Bands," *Ieee Transactions on Antennas and Propagation*, vol. 62, pp. 2430-2439, May 2014.

[23] IEEE Std C95.1™-2005, "IEEE Standard for Safety Levels with respect to Human exposure for RF electromagnetic fields 3 kHz to 300 GHz," *IEEE International Committee on Electromagnetic Safety (SCC39)*, April 2006.

[24] R. S. Alrawashdeh, Y. Huang, M. Kod, and A. A. Sajak, "A Broadband Flexible Implantable Loop Antenna With Complementary Split Ring Resonators," *Ieee Antennas and Wireless Propagation Letters*, vol. 14, pp. 1506-1509, 2015.